European Journal of Pain

ORIGINAL ARTICLE

Individualised Alpha-tACS for Modulating Pain Perception and Neural Oscillations: A Sham-Controlled Study in Healthy Participants

Yaser Fathi[1] | Françoise Dissassuca[1] | Gloria Ricci[1,2] | Giulia Liberati[1,3]

[1]Institute of Neuroscience, Université Catholique de Louvain, Brussels, Belgium | [2]Department of Neuroscience, University of Padova, Padova, Italy | [3]Psychological Sciences Research Institute, Université Catholique de Louvain, Louvain-la-Neuve, Belgium

Correspondence: Yaser Fathi (yaser.fathiarateh@uclouvain.be)

Received: 27 March 2025 | **Revised:** 20 June 2025 | **Accepted:** 5 July 2025

Funding: Y.F. is supported by a MIS grant from the FNRS. G.L. is supported by FNRS and Fondation Médicale Reine Elisabeth (FMRE) grants.

Keywords: individual alpha frequency (IAF) | neural oscillations | nociception | pain perception | transcranial alternating current stimulation (tACS)

ABSTRACT

Background: Neural oscillations are increasingly recognised as key mechanisms integrating the sensory, affective and cognitive dimensions of pain, yet their precise role in pain modulation remains poorly understood. Transcranial alternating current stimulation (tACS) offers a promising tool for modulating these oscillations and elucidating their function in pain processing. However, findings on tACS-induced pain modulation have been inconsistent, possibly due to a lack of individualised protocols.

Methods: In this study, we investigated the effects of tACS delivered at the individual peak alpha frequency (IAF) on both pain perception and neural oscillations. Using a within-subject, sham-controlled design, we applied tACS over the primary motor cortex (M1) contralateral to the dominant arm in 38 healthy participants. Sustained periodic 0.2 Hz thermonociceptive stimuli were applied to the dominant forearm before and after tACS. Pain perception and heat pain thresholds (HPT) were assessed before and after tACS. To calculate IAF from recorded scalp electroencephalography, we used a discriminative approach based on independent component analysis, enabling the isolation of somatosensory IAF (SS-IAF).

Results: The results revealed an overall increase in pain perception and a decrease in HPT in both sham and active conditions, with no significant interactions between conditions. However, a trend toward reduced sensitisation to thermonociceptive stimuli post-tACS was observed. Exploratory analyses suggested a sex-specific effect of tACS, with a potential modulation of HPT observed in women but not in men. Furthermore, we observed a significant correlation between SS-IAF and HPT.

Conclusions: These findings provide novel perspectives on advancing individualised neuromodulation approaches for pain.

Significance: This article introduces an individualised transcranial alternating current stimulation (tACS) approach, targeting the sensorimotor area at the individual somatosensory alpha frequency. Our findings highlight its potential for modulating pain perception and provide novel perspectives on advancing individualised neuromodulation for pain management.

1 | Introduction

Evidence from previous studies suggests that neural oscillations may serve as mechanisms facilitating the integration of sensory and cognitive processes, which could be relevant to chronic pain (Furman et al. 2019; Huneke et al. 2013; Liberati, Klöcker, Algoet, et al. 2018; Liberati, Algoet, Ferrao Santos, et al. 2018; Mazaheri et al. 2022; McLain et al. 2022; Ploner et al. 2017).

Brain alpha activity has been linked to pain perception through both its amplitude and frequency characteristics. Alpha power—measured during noxious stimulation or at rest—has been shown to be negatively correlated with pain ratings (Nir et al. 2012). Moreover, alpha amplitude can be modulated by cognitive and contextual factors, as it decreases with attention to pain (May et al. 2012) and increases with the expectation of pain relief (Huneke et al. 2013). In addition, the frequency of alpha oscillations might also play a role in pain inhibition or facilitation. A slowing of the individual peak alpha frequency (IAF) has been observed in those suffering from chronic pain (Furman et al. 2019; Sarnthein et al. 2006; de Vries et al. 2013; Walton et al. 2010). IAF has also been shown to predict pain sensitivity in healthy individuals (Furman et al. 2018). Recent findings suggest that slower IAF may reflect greater nociceptive facilitation (Huber et al. 2025).

Transcranial alternating current stimulation (tACS) could provide new opportunities for understanding and manipulating these oscillatory activities. tACS has been suggested to entrain neuronal activity, aligning its phase with the stimulation frequency, when applied at the endogenous frequency (Ali et al. 2013; Huang et al. 2021). tACS may also facilitate synaptic plasticity through spike-timing dependent plasticity (STDP), which could in turn enhance the power of alpha oscillations (Vossen et al. 2015). Applying tACS at IAF has been proposed to increase the likelihood of effective neuronal synchronisation (Riddle and Frohlich 2021), stabilise IAF against potential slowing and possibly enhance its power and gating functions. While the idea of enhancing alpha power to modulate pain perception has been investigated previously with heterogeneous results (Arendsen et al. 2018; Hohn et al. 2025), the idea of enhancing IAF or preventing its slowing has been less explored. Interindividual differences in IAF highlight the need for individualised interventions, as fixed stimulation protocols may increase variability in outcomes.

We employed individualised tACS at IAF over the sensorimotor cortex of healthy participants to investigate its effects on pain perception and neural oscillations. Sensorimotor cortex has a central role in integrating nociceptive and motor processes (Murray and Sessle 2024). We used a discriminative approach to separate somatosensory-related independent components (ICs) of the IAF from visual-related components. Then we utilised these components to reconstruct EEG signals and identify the somatosensory IAF (SS-IAF). Sustained periodic thermonociceptive stimuli were delivered both before and after tACS. Behavioural responses—including stimulus intensity, painfulness rate (i.e., the number of thermonociceptive stimuli that were perceived as painful), warm detection threshold (WDT) and heat pain threshold (HPT)—were recorded. We hypothesised that tACS at the selected IAF: (i) modulates pain perception and (ii) alters pain-related ongoing oscillatory responses.

2 | Method

2.1 | Participants

Sample size: We conducted a simulation-based power analysis to determine the required sample size based on Linear Mixed Models (LMM) analysis with the regression formula: Measurement ~ Condition * Time + (1|Participant) with power of 0.9, and alpha level of 0.05. Using pilot data of HPT, we assumed a baseline mean HPT of 46.7°C and a standard deviation (SD) of 4.3°C, applied for each condition and time point. A medium interaction effect size ($f = 0.25$) was assumed, corresponding to an estimated mean difference of approximately 2.15°C in the postactive condition ($\Delta\mu \approx 2.f.SD$). Starting with an initial sample size of 25 participants, simulations iteratively tested varying sample sizes (repeated 1000 times per sample size) to determine the smallest sample size required to achieve power of 0.9, at a significance level of 0.05. This approach resulted in a recommended sample size of 38 participants.

We recruited 40 participants to account for potential dropouts; due to technical issues, data collection was incomplete for two individuals, resulting in a final dataset of 38 participants (19 females, 19 males; age: 28 ± 8.5). All experimental procedures were approved by the local Research Ethics Committee (AAHRPP-DSQ-037) and were performed in compliance with the Code of Ethics of the World Medical Association (Declaration of Helsinki). Prior to the experiment, all participants were informed about the procedure and potential side effects and provided written informed consent. Participants received a financial compensation of 10 euros per hour.

The inclusion criterion for participants was being over 18 years old. The exclusion criteria included pregnancy, history of seizures or epilepsy, severe head injury, neurological or psychiatric illness, cardiac or respiratory conditions, metal implants in the head or scalp, cochlear implants, cardiac pacemakers, implanted neurostimulators (e.g., cortical, cerebral, vagus nerve, spinal cord) and implanted drug delivery devices.

2.2 | Experiment Design

We designed a within-subject double-blind experiment in which each participant completed two sessions (sham and active tACS), separated by approximately 7 days, to minimise carryover effects (Figure 1). The experiment followed a 2 × 2 design, with factors being condition (sham, active) and time (pre, post). The order of the sessions was counterbalanced across participants. Each session followed a structured protocol. The first step allowed participants to familiarise themselves with thermonociceptive stimuli. This familiarisation phase consisted of three thermonociceptive stimuli with peak amplitudes similar, but not identical, to those used in the main experiment.

Next, participants completed 4 min of rest during which EEG was recorded (2 min during eyes closed and 2 min during eyes open), and 10 trials of 1-min sustained thermonociceptive stimulation. The order of these tasks was randomised and counterbalanced across participants but remained consistent for pre- and post-tACS measurements. Furthermore, the same order was maintained for sham and active tACS sessions for each participant. The IAF was then computed using a custom MATLAB program (detailed in the IAF calculation section below), which took approximately 5 min. During this time, we also measured the warm detection threshold (WDT) and heat pain threshold (HPT). Participants then underwent 20 min of either sham or active tACS. Following tACS, the same procedures as before were repeated, beginning with WDT and HPT measurements. This

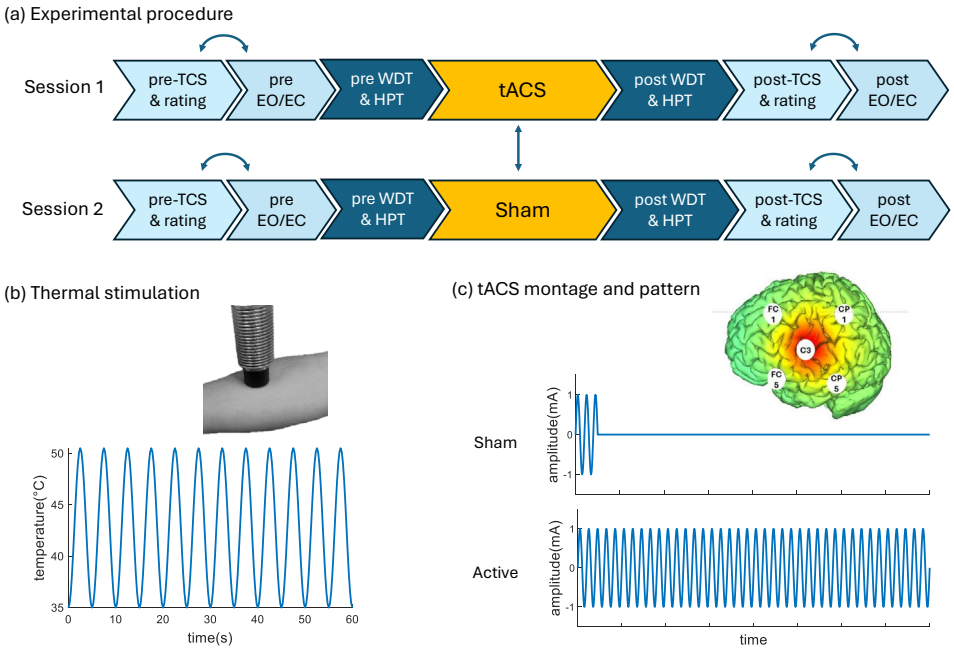

FIGURE 1 | Paradigm of the experiment. (a) Timeline of the experimental protocol for active and sham tACS sessions. Blue arrows indicate that the order was randomised across participants. (b) Illustration of thermal cutaneous stimulation (TCS) applied to the forearm with a sinusoidal temperature waveform. (c) High-definition 4×1 tACS montage targeting the primary motor cortex (M1), and stimulation patterns for sham and active conditions. EC, eyes closed; EO, eyes open; TCS, thermal cutaneous stimulation.

was followed by 4 min of resting EEG (2 min eyes closed, 2 min eyes open), and 10 trials of 1 min sustained periodic thermonociceptive stimulation.

2.3 | Sustained Thermonociceptive Stimulation

To better understand how pain is related to neural oscillations, we used a long-lasting 1-min, periodically modulated stimulus (12 sin cycle with a frequency of 0.2 Hz) also used in previous studies (Colon et al. 2017; Liberati et al. 2019). In previous scalp EEG studies, it has been shown that this type of stimulation modulates ongoing neural oscillations at the frequency of stimulation (Colon et al. 2017; Liberati et al. 2019). Moreover, the perception of sustained pain has been associated with changes in the magnitude of modulated ongoing oscillations (Colon et al. 2017; Liberati et al. 2019). Thermonociceptive stimuli were delivered on the volar forearm of the dominant arm of the participant using a thermal cutaneous stimulator (TCS, QST Lab), set with 15 micro-Peltier elements (each with an approximate area of 7.7 mm^2) whose temperature varies at rates of up to 300°C/s. The temperature of stimulation varied between a baseline temperature (35°C) and 50.5°C in a sinusoidal fashion. These parameters are known to elicit pain in the great majority of individuals (Leu et al. 2023; Mulders et al. 2020) and were also tested in pilot experiments before starting the main experiment. The stimulation probe was slightly displaced after each trial to limit sensitisation.

2.4 | Behavioural Measurements

After each of the 10 sustained periodic thermonociceptive stimulations, participants were prompted to rate their perception in response to a question displayed on the screen: 'How intense did you perceive the stimulation?' (scale: 0–10, where 0 indicated 'no perception', and 10 indicated the 'highest intensity imaginable'). In addition, participants were required to respond to 'Did you perceive the stimulation as painful?' (yes/no). The intensity ratings were averaged across the 10 trials, and the pain perception responses (0 for 'no' and 1 for 'yes') were summed to provide a painfulness rate for each session.

For threshold measurements, participants were seated with their arm resting on a desk while a thermode (TCS, QST Lab) was applied to the forearm of their dominant hand. The temperature started at 27°C and increased at a rate of 1°C per second, with a maximum limit of 50°C. Without being able to see the temperature, participants were instructed to focus on their perception and press a button with their other hand as soon as they felt the slightest warming sensation (for warm detection threshold, WDT) and, subsequently, the first sensation of pricking or burning (for heat pain threshold, HPT). It was emphasised that the goal was to detect the initial sensation of heat pain, not to measure heat pain tolerance. WDT was measured before HPT to progress from less to more intense stimuli, reducing confounds such as sensitisation or desensitisation. Each measurement was repeated three times, and the average value was used for analysis.

2.5 | EEG Recording

EEG data were recorded using the same Starstim 32 system (Neuroelectrics, Barcelona, Spain) employed for tACS. For EEG recording, we used 32 Ag/AgCl electrodes based on the International 10-10 system with a DRL (Driven Right Leg) and CMS (Common Mode Sense) attached to the earlobe. EEG was

recorded at a 500 Hz sampling rate during thermonociceptive stimulation and rest periods with eyes open and eyes closed, both before and after tACS. Electrode impedances were maintained below 20 kΩ. The recorded data were stored for offline processing.

2.5.1 | Preprocessing

The recorded signals were first preprocessed, including bandpass filtering (0.05–45 Hz) of signals recorded during TCS, EC and EO using a 4th-order Butterworth filter and segmented into 1-min trials. After detrending and mean removal, signals were re-referenced to the average of all channels. Wavelet ICA was then applied to automatically remove or suppress movement-related artefacts (Castellanos and Makarov 2006; Jordan Sorokin 2025). For left-handed participants ($n = 2$), channels were symmetrically reordered across hemispheres (e.g., C4 for C3) to ensure consistent interpretation and analysis.

2.5.2 | IAF Determination (Online Processing)

To measure the IAF, we employed an ICA-based method developed by Lebrun et al. (2025) to dissociate vision-related alpha-band activity (VIS-alpha) and somatosensory alpha-band activity (SS-alpha commonly associated with mu rhythm activity). Since central mu rhythms often overlap with posterior alpha sources (Garakh et al. 2020), we aimed to isolate the alpha component specifically modulated by pain-related input. An ICA was used to decompose the EEG signals recorded during the rest eyes closed (EC), rest eyes open (EO) and TCS-stimulation conditions into 31 components. The classification of ICs involved two main steps. First, using the average of the frequency spectra obtained in all three conditions (EC, EO and TCS), potential alpha-band activity captured by each IC was identified by computing the peak frequency within the 7–13 Hz range using the centre of gravity (CoG) formula:

$$\mathrm{CoG} = \frac{\sum_{i=1}^{n} f_i a_i}{\sum_{i=1}^{n} a_i}$$

where f_i is the ith frequency bin, a_i is the spectral amplitude for f_i, and n is the number of bins in the 7–13 Hz range. A 6 Hz frequency window centred on the CoG was then defined. Within this window, the mean amplitude and standard error of the mean (SEM: standard deviation of amplitudes divided by the square root of the number of bins) were computed separately for each condition. Confidence intervals were derived as mean ± SEM for each condition. These confidence intervals were then used to define the lower and upper bounds of the alpha power spectrum for each of the three conditions (EO, EC and TCS). Based on these bounds, ICs were categorised using the criteria described in Algorithm 1 below:

In summary, ICs were categorised into four groups:

1. *Somatosensory-ICs* (*SS-ICs*): Components displaying a decrease in alpha amplitude during thermal cutaneous stimulation (TCS) without modulation by eyes-open (EO) or eyes-closed (EC) conditions.
2. *Visual-ICs* (*VIS-ICs*): Components with higher alpha amplitude in EC compared to EO and TCS, but not sensitive to TCS.
3. *MIX-ICs* Components showing an increase in alpha amplitude in EC relative to EO and a decrease during TCS compared to EO.
4. *None*: Cases where the algorithm could not classify ICs into the above categories.

Figure 2 shows examples of SS-ICs and VIS-ICs under different recording conditions. EEG signals were reconstructed using ICs from each category, and the IAF was determined based on the centre of gravity (CoG) within the 7–13 Hz range. The peak of alpha wave frequency at C3 (or C4 for left-handed participants) was designated as the IAF. Priority was given to IAF extracted from EEG reconstructed by SS-ICs, followed by MIX-ICs, then VIS-ICs. If no components matched these categories, a standard value of 10 Hz corresponding to the average peak frequency across subjects (May et al. 2012) was chosen for tACS stimulation. This approach is similar to the one described by Gundlach et al. (2017), where somatosensory-related alpha frequencies were derived from recordings during passive somatosensory stimulation.

2.6 | Transcranial Alternating Current Stimulation (tACS)

tACS at the IAF was delivered for 20 min to the primary motor cortex (M1) using a 32-channel tES-EEG device (Starstim 32, Neuroelectrics, Barcelona, Spain). This device enabled EEG recording and electrical stimulation within a single setup. Once the neuroprene headcap was in place, EEG signals could be recorded, and brain stimulation could be delivered to specific targets by selecting the corresponding electrodes.

ALGORITHM 1 | Algorithm to Label Independent Components.

1 **Input**: Lower and upper bounds of the IC power spectrum in each condition (EO_{LB}, EO_{UB}, EC_{LB}, EC_{UB}, TCS_{LB}, TCS_{UB}).
2 **Output**: Classification label for each IC (*SS-IC, VIS-IC, MIX-IC, None*).
3 **Conditions:**
(C1) TCS suppression: $TCS_{UB} < EO_{LB}$ & $TCS_{UB} < EC_{LB}$.
(C2) EO–EC overlap: $EC_{LB} < EO_{UB}$ & $EO_{LB} < EC_{UB}$.
(C3) EC enhancement: $EC_{LB} > EO_{UB}$ & $EC_{LB} > TCS_{UB}$.
(C4) EO–TCS overlap: $TCS_{LB} < EO_{UB}$ & $EO_{LB} < TCS_{UB}$.
(C5) TCS suppression + EC enhancement: $TCS_{UB} < EO_{LB}$ & $EC_{LB} > EO_{UB}$.
4 Classification rules: (for each IC)
If (C1) and (C2) → classify as *SS-IC*.
If (C3) and (C4) → classify as *VIS-IC*.
If (C5) → classify as *MIX-IC*.
Otherwise → classify as *None*.

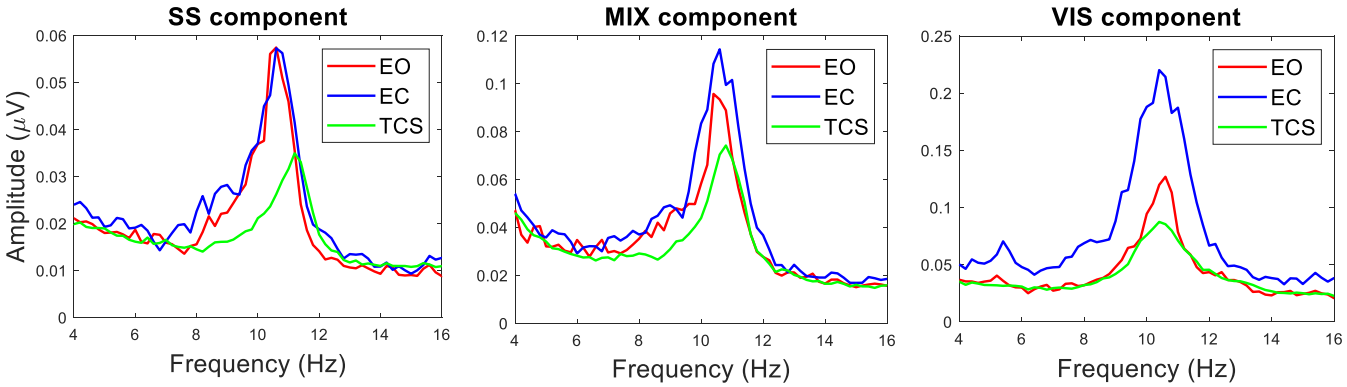

FIGURE 2 | Classification of ICs into SS, VIS and MIX categories based on their alpha-band activity. Frequency spectra showing the SS-IC (left), MIX-IC (middle) and VIS-IC (right) under different conditions: eyes open (EO), eyes closed (EC) and thermal cutaneous stimulation (TCS). The VIS component exhibited higher alpha amplitude during the EC condition compared to EO and TCS, whereas the SS component showed reduced alpha amplitude during TCS compared to EO or EC conditions.

We applied a high-definition 4×1 montage to achieve focal stimulation (Figure 1C). A sine-wave electrical current with a peak amplitude of 1 mA (zero to peak) was delivered to M1 contralateral to the nociceptive stimulation. The centre of stimulation was electrode C3 (or C4 for left-handed participants), surrounded by four electrodes positioned in a ring approximately 5 cm away at FC1, FC5, CP1 and CP5 (or FC2, FC6, CP2 and CP6 for left-handed participants) to enhance focality. The surrounding electrodes received 25% of the total current. We used Ag/AgCl based electrodes, each with a surface area of 3.14 cm^2.

For sham stimulation, the protocol included a 30-s ramp-up followed by a 30-s ramp-down at the beginning of the session. This procedure was chosen in order to mimic the initial sensations of real tACS, reducing expectation biases. At the end of each session, participants answered three questions assessing their sensory experiences related to the stimulation. They rated the intensity of tingling or pricking sensations perceived on the scalp (0–10, with 10 being the most intense imaginable) and the intensity of perceived light flickering sensations (0–10, with 10 being the most intense imaginable). Additionally, they indicated whether they believed they had received continuous stimulation (yes/no). The order of sham and active stimulation was randomised for each participant and uploaded to the stimulation device via MATLAB scripts. Both the participant and the operator were blinded to the stimulation protocol.

2.7 | EEG Data Analysis (Offline Processing)

2.7.1 | IAF Offline Analysis

In addition to the online calculation of IAF used to determine the frequency of stimulation, we conducted post hoc analyses to compare IAF pre- and poststimulation. The data were preprocessed as described in the online IAF calculation section, including bandpass filtering, re-referencing and artefact removal. The same component classification procedure (SS-IC, VIS-IC, MIX-IC) was applied, and IAF was determined for each condition (pre- and poststimulation) using the centre of gravity (CoG) method. This allowed for a direct comparison of changes in IAF induced by tACS. A schematic representation of the preprocessing and analysis steps is presented in Figure 3.

2.7.2 | Frequency Tagging Analyses

We used periodic thermonociceptive stimuli to modulate neural ongoing oscillations at the frequency of stimulation, enabling us to analyse their modulation in relation to pain perception. To analyse these oscillatory responses, we used a frequency tagging (FT) approach, a method that isolates neural activity synchronised with the frequency of the periodic stimuli, allowing us to track amplitude-specific changes in the brain's response to thermonociceptive input.

We analysed both the phase-locked response at the frequency of stimulation and the modulation of ongoing oscillatory activity in the different frequency bands at the same frequency. The data were initially preprocessed as described in the above section on IAF calculations. For the phase-locked responses, after preprocessing and segmentation of EEG signals into the 1-min epochs, we averaged data over epochs for each participant and each condition and then transformed them to the frequency domain using a Fourier transform. Using this frequency domain analysis approach, we expect to see distinct peaks in the EEG frequency spectrum at the stimulation frequency and its harmonics. To better estimate the response amplitude at each frequency bin, we subtracted the average amplitude of the signal measured at neighbouring frequencies (−0.026 to −0.065 and 0.026 to 0.065 Hz) to reduce residual noise (Liberati et al. 2019).

The signal-to-noise ratio (SNR) for each harmonic was defined as the ratio of harmonic power to baseline noise power and calculated as:

$$\mathrm{SNR} = 10 \times \log \frac{P_{\mathrm{harmonic}}}{P_{\mathrm{baseline\ noise}}} = \left(\frac{A_{\mathrm{harmonic}}}{A_{\mathrm{baseline\ noise}}} \right)^2$$

where A_{harmonic} represents the amplitude at each harmonic, and $A_{\mathrm{baseline\ noise}}$ is the average amplitude of the signal at neighbouring frequencies (−0.026 to −0.065 and 0.026 to 0.065 Hz), as defined above. We aggregated harmonics whose SNR, averaged across

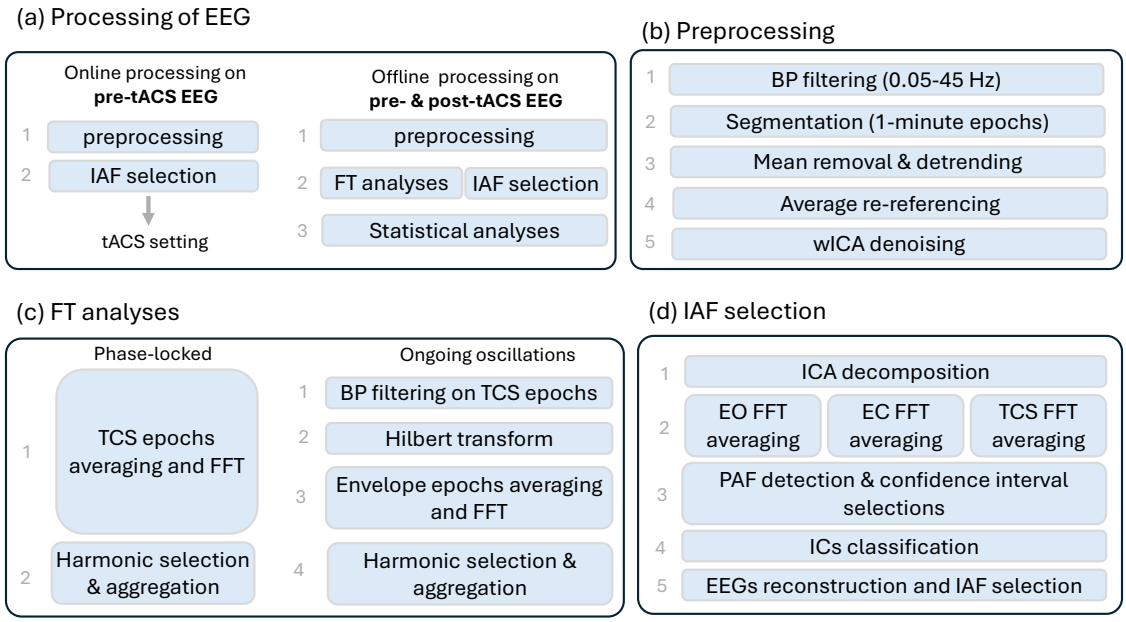

FIGURE 3 | Overview of the EEG processing pipeline. (a) Processing of EEG signals includes both online and offline analyses. Online processing of pre-tACS EEG involves preprocessing and IAF selection, which guides tACS settings. Offline processing of pre- and post-tACS EEG includes preprocessing, frequency tagging (FT) analyses, IAF selection and statistical analyses. (b) Preprocessing steps include bandpass filtering (0.05–45 Hz), segmentation into 1-min epochs, mean removal, detrending, average re-referencing and Wavelet ICA (wICA) denoising to remove artefacts. (c) FT analyses are divided into two components: Phase-locked responses (averaging TCS epochs, Fourier Transform and harmonic selection/aggregation) and ongoing oscillatory activity (bandpass filtering, Hilbert transform for envelope extraction, averaging and harmonic aggregation). (d) IAF selection workflow, consisting of ICA decomposition, averaging FFT for EO, EC and TCS conditions, detection of IAF and confidence intervals, IC classification (SS-IC, VIS-IC, MIX-IC) and reconstruction of EEG signals to finalise IAF for tACS stimulation.

all channels, was greater than zero. Aggregated amplitudes were used for statistical tests.

For analysing the ongoing oscillatory response to periodic stimuli, a similar procedure was applied. After preprocessing and segmenting the EEG signals into epochs, the signals were bandpass filtered into theta (4–8 Hz), alpha (8–13 Hz) and beta (13–30 Hz) frequency bands consistent with COBIDAS guidelines (Pernet et al. 2020) using Butterworth bandpass filters. The signal envelopes within each band were then extracted using the Hilbert transform. Finally, the envelopes were averaged across epochs for each participant and condition and transformed into the frequency domain using the Fourier transform. Residual noise correction and SNR calculation for harmonics were performed similarly to the approach used previously for phase-locked responses.

2.8 | Statistical Analyses

Statistical analyses were conducted using LMMs with the fitlme function in MATLAB (2023a, The MathWorks). The model was fitted using restricted maximum likelihood (REML), ensuring robust estimation of both fixed and random effects.

Residuals of the LMM were checked for normality using both a Q–Q plot and the Shapiro–Wilk test. If residuals were not normal, skewness was evaluated. For skewness values greater than 0.5, a log transformation was applied to normalise the data. Outliers were then identified using Cook's distance, and the sample with the highest Cook's distance was removed if it exceeded a threshold of 3 standard deviations of the distance. The model was then refitted, and residuals were reassessed. If residuals still showed non-normality, the outlier removal process was repeated. This procedure was limited to a maximum of 5% of the dataset to ensure no more than 5% of data was removed. Normality was achieved in all cases before exceeding the 5% data removal limit.

2.8.1 | Behavioural Responses

To examine the effect of tACS on behavioural responses, we performed four LMM analyses with the following model: Measurement ~ Condition * Time + (1 | Participant), where Measurement refers to the dependent variable, which varied based on the analysis (HPT, WDT, painfulness rate or intensity ratings). Condition (sham vs. active) and Time (pre- vs. post-stimulation) were included as fixed effects, along with their interaction. Random intercepts were specified for Participant to account for between-subject variability.

2.8.2 | Phase-Locked and Ongoing Oscillations Responses

As described earlier, aggregated amplitudes of harmonics with SNR higher than zero were used for statistical tests. We used a permutation-based significance test to identify the channel with the most significant modulations across all conditions, testing whether the peak aggregated amplitudes at each channel were significantly greater than zero (Leu et al. 2024). First,

a one-tailed Wilcoxon signed-rank test was applied to each channel to assess whether its values differed significantly from zero. To account for multiple comparisons across the four conditions (sham vs. active, pre- vs. poststimulation), we applied a Bonferroni-corrected threshold of $\alpha = 0.05/4 = 0.0125$. A null distribution was generated by randomly flipping the signs of the data in 2000 permutations. Channels were regarded as significant if their p values were below the threshold and their count exceeded the 95th percentile of the null distribution, ensuring robust control of false positives. We selected the most significant channel with the highest test statistic for further analyses.

To see the tACS effect on phase-locked responses, we performed LMM analyses with the following formula: Measurement ~ Condition * Time + (1 | Participant), where Measurement refers to the aggregated amplitude of the phase-locked FT response at the most significant channel. For ongoing oscillations, we used the same model (Measurement ~ Condition * Time + (1 | Participant)) and analyses, but here Measurement referred to the aggregated amplitude of the ongoing oscillations' FT response in the theta, alpha or beta frequency bands, with the most significant channel determined separately for each band.

2.8.3 | IAF Data

To evaluate the IAF data, we performed LMM analyses using the same model, with IAF as the dependent variable and condition, time and their interaction as fixed independent factors, and participants as a random factor.

2.8.4 | Blinding

To assess blinding we analysed responses to the first two questions (perceived intensity of tingling at scalp and light flickering) using Wilcoxon signed-rank tests, and the third question using a Cochran's Q-test. Participants responses from both sham and active conditions were used for these analyses.

3 | Results

3.1 | Sensations Related to Active and Sham tACS

Participants' ratings of scalp sensations were significantly higher in the active compared to the sham condition ($p = 0.00005$), with average ratings of 5.1 and 2.6, respectively. Flickering sensations were reported by a small number of participants ($n = 9$ in the active condition, with a mean rating of 3.6, and $n = 4$ in the sham condition, with a mean rating of 3.5), but there was no significant difference between conditions ($p = 0.99$). Finally, Cochran's Q-test on responses to the third question revealed a significant difference between sham and active conditions ($p = 0.0004$): 28 out of 38 participants reported receiving continuous stimulation during the active condition, whereas only 5 participants reported the same during the sham condition.

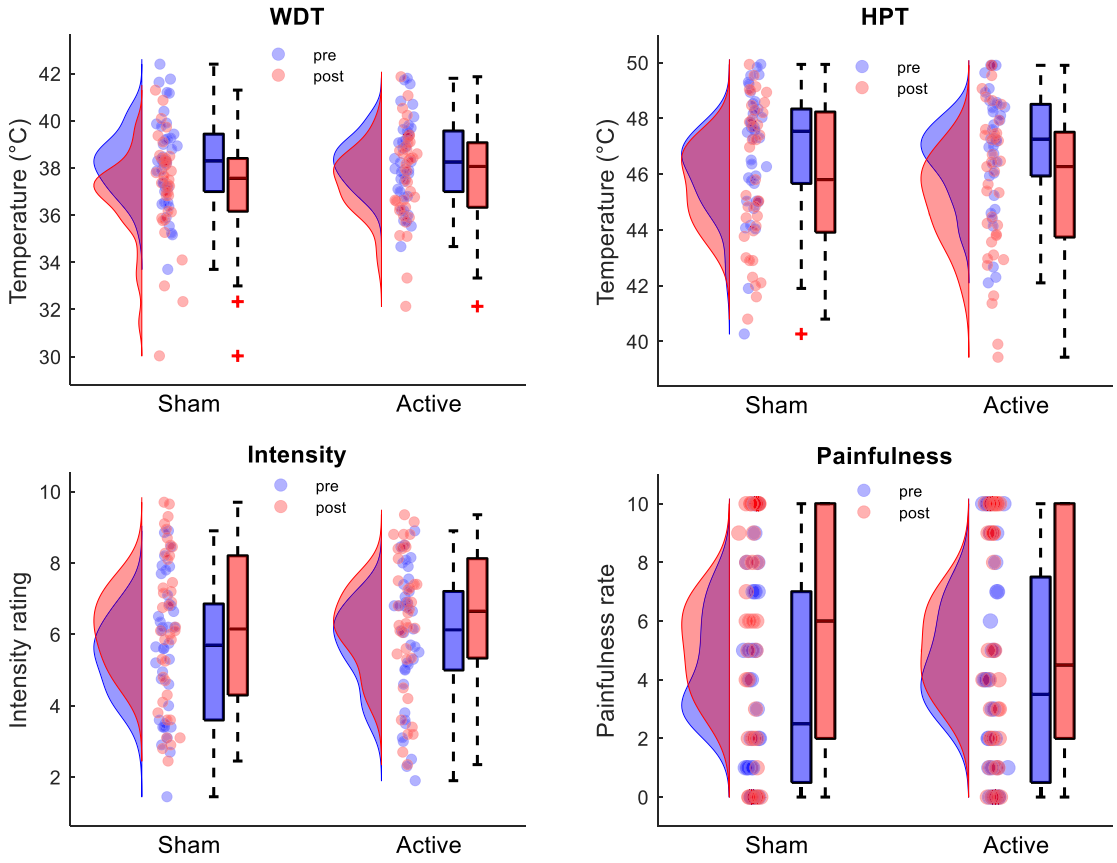

FIGURE 4 | Variations in WDT, HPT, stimulus intensity ratings and painfulness rates across different conditions and time points for all participants. LMM results for all measurements show a significant effect of time for all measurements.

3.2 | Behavioural Responses

The results of behavioural measurements for all participants at different conditions and time points are shown in Figure 4. The LMM results for behavioural measures indicate a significant decrease in WDTs ($F = 9.5$; $p = 0.002$) and HPTs ($F = 11.7$; $p = 0.0007$) for both postactive and postsham conditions, with no significant interaction between time and condition ($F = 0.8$; $p = 0.35$ for WDT; $F = 0.1$; $p = 0.78$ for HPT). Additionally, participants showed a significant increase in perceived stimulus intensity during sustained periodic stimulation ($F = 22.7$; $p < 0.0001$), as well as an increase in the painfulness rate ($F = 17.9$; $p < 0.0001$). These consistent decreases in thresholds and increases in perceived intensity ratings may reflect mild sensitisation resulting from sustained thermal stimulation.

Figures also show that the average decrease in WDT and HPT, as well as the increase in intensity and painfulness rate, was less pronounced in the active tACS condition compared to sham. The average decrease in WDT and HPT was 1.1°C for sham and 0.6°C for tACS, while the average increase in painfulness rate on a 0–10 scale was 0.16 for sham and 0.11 for tACS. For intensity on a 0–10 scale, the average increase was 0.61 for sham and 0.51 for tACS. However, statistical analyses indicate that these differences did not result in significant interactions (see Table S1).

3.3 | Neural Responses to Sustained Periodic Thermonociceptive Stimulation

The results of the Wilcoxon signed-rank test showed that the strongest phase-locked periodic modulation across all conditions and time points occurred at FC2. For ongoing oscillations, the test revealed that the strongest periodic modulation was at Cz for the theta frequency band and at C3 for the alpha and beta frequency bands, respectively (Figure 5). The results of each condition and time point can be found in Figure S2.

In Figure 6, the frequency spectra at the most significant electrodes, averaged across participants, illustrate the neural

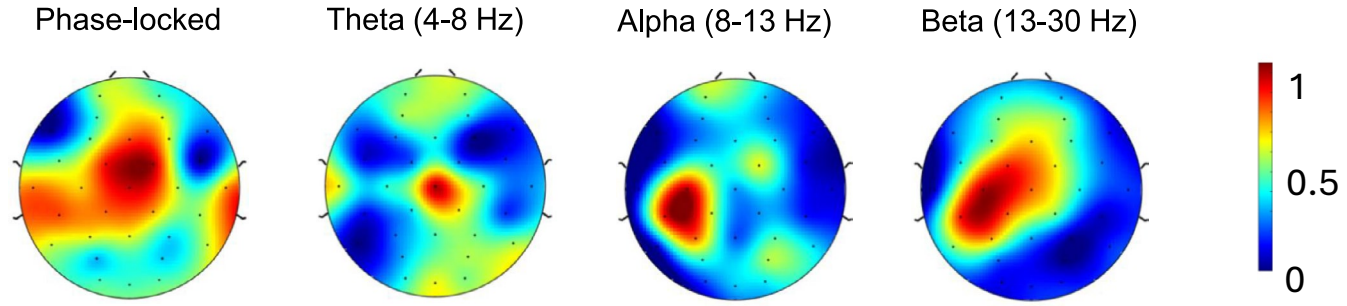

FIGURE 5 | Topographical maps showing the strongest phase-locked activity and ongoing oscillatory modulations in response to periodic thermonociceptive stimulation considering all conditions and time points together. The phase-locked response is localised at FC2, while ongoing oscillatory activity shows the strongest modulations at Cz for the theta band (4–8 Hz) and at C3 for the alpha (8–13 Hz) and beta (13–30 Hz) bands. Colour scales represent Wilcoxon test statistics.

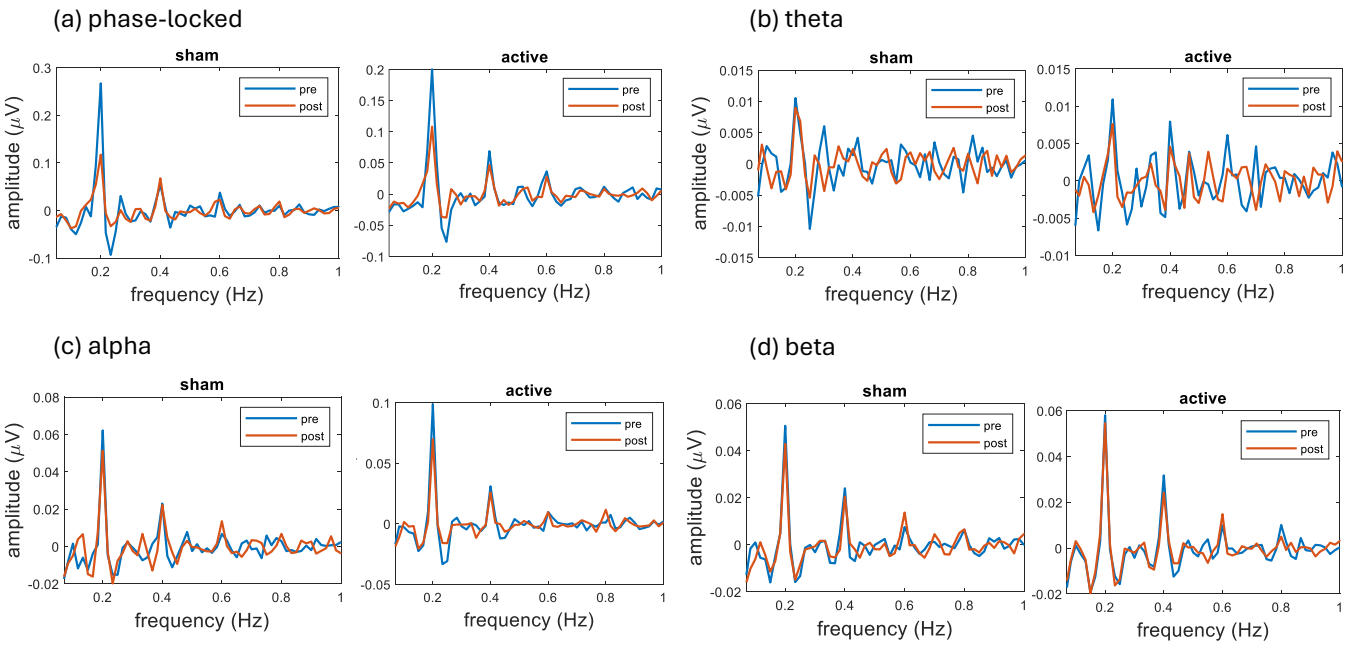

FIGURE 6 | Frequency domain representation of phase-locked and oscillatory activity in response to periodic thermonociceptive stimulation averaged across all participants. (a) Phase-locked, (b) theta-band oscillations, (c) alpha-band oscillations and (d) beta-band oscillations are shown separately for sham and active conditions. Prestimulation (blue) and poststimulation (red) spectra highlight changes in amplitude across conditions.

phase-locked and oscillatory responses to periodic thermonociceptive stimulation under different conditions and time points. The spectra show decreased amplitudes in poststimulation compared to prestimulation, with a more pronounced reduction in the phase-locked response. LMM analyses for phase-locked responses showed that there was a significant time effect ($F = 5.0$; $p = 0.03$), but no condition effect or interactions between time and condition (see Table 1). The analyses of ongoing oscillations at theta, alpha and beta showed no significant time, condition or interaction effect on periodic modulations (Table 1). Figure 7 shows the distribution and boxplots of aggregated harmonic amplitudes for phase-locked responses, theta, alpha and beta bands across sham and active conditions. A decrease in amplitudes poststimulation compared to prestimulation is observed for phase-locked responses, while other frequency bands do not show a consistent change.

3.4 | IAF Analyses

SS-IAF was detected in 26 subjects, VIS-IAF was detected in three subjects, and MIX-IAF was detected in seven subjects; in the remaining two subjects, none of these three specific ICA-based IAF were detected, so 10 Hz was selected as a default tACS

TABLE 1 | Results of statistical tests for phase-locked and ongoing oscillations at the channel with the most significant amplitude modulations by thermonociceptive stimulation: phase-locked (FC2), theta (Cz), alpha (C3) and beta (C3).

	Phase-locked (FC2)	Theta (Cz)	Alpha (C3)	Beta (C3)
Condition	$F = 0.5$, $p = 0.47$	$F = 0.0$, $p = 0.92$	$F = 1.9$, $p = 0.17$	$F = 0.2$, $p = 0.69$
Time	$\mathbf{F = 5.0}$, $\mathbf{p = 0.03}$	$F = 0.15$, $p = 0.69$	$F = 0.1$, $p = 0.80$	$F = 3.0$, $p = 0.09$
Interaction	$F = 0.4$, $p = 0.54$	$F = 0.1$, $p = 0.76$	$F = 0.2$, $p = 0.67$	$F = 2.0$, $p = 0.16$

Note: Bold values indicate $p < 0.05$.

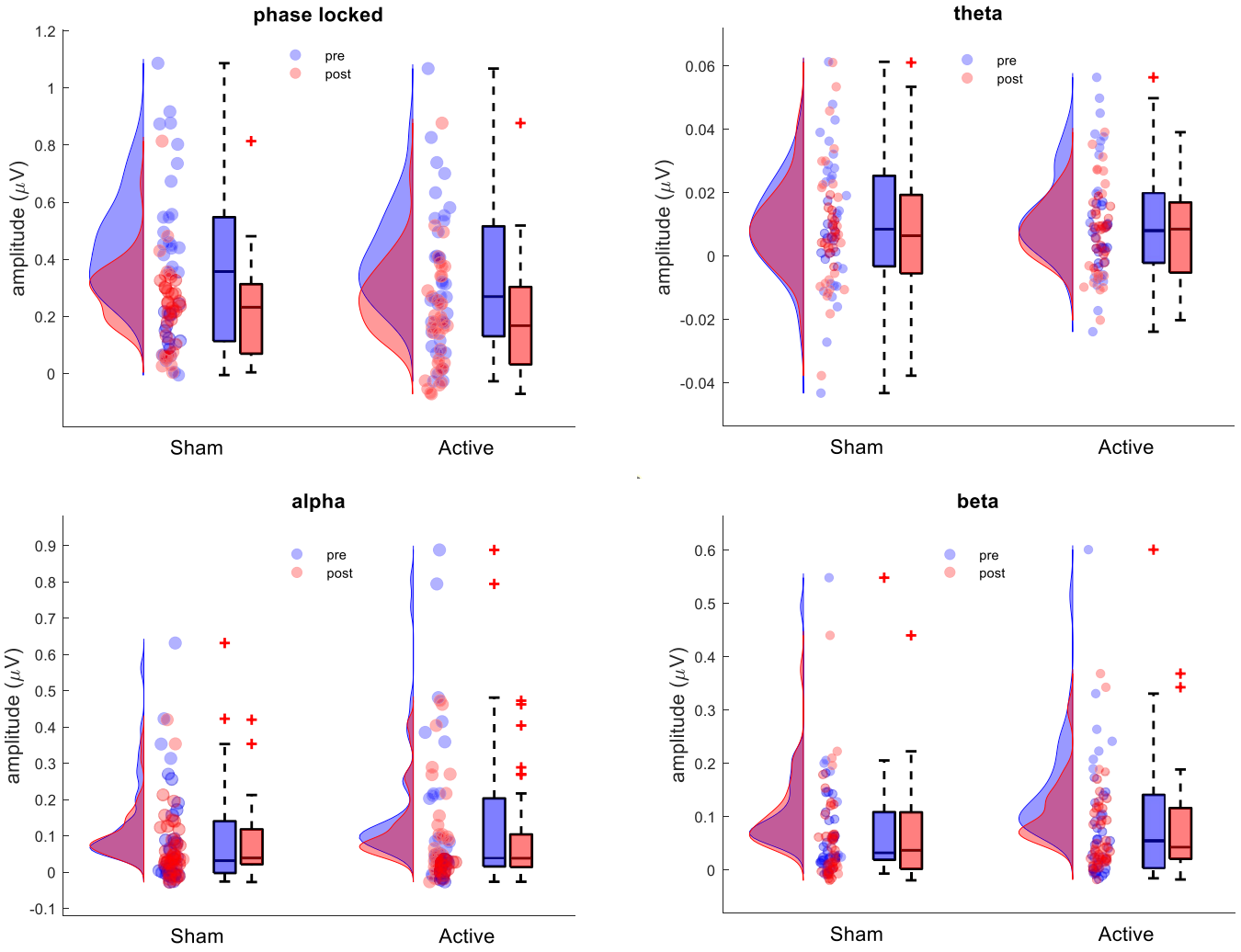

FIGURE 7 | Distributions and boxplots of amplitudes across participants for phase-locked responses (top left), theta band (top right), alpha band (bottom left) and beta band (bottom right) during sham and active conditions.

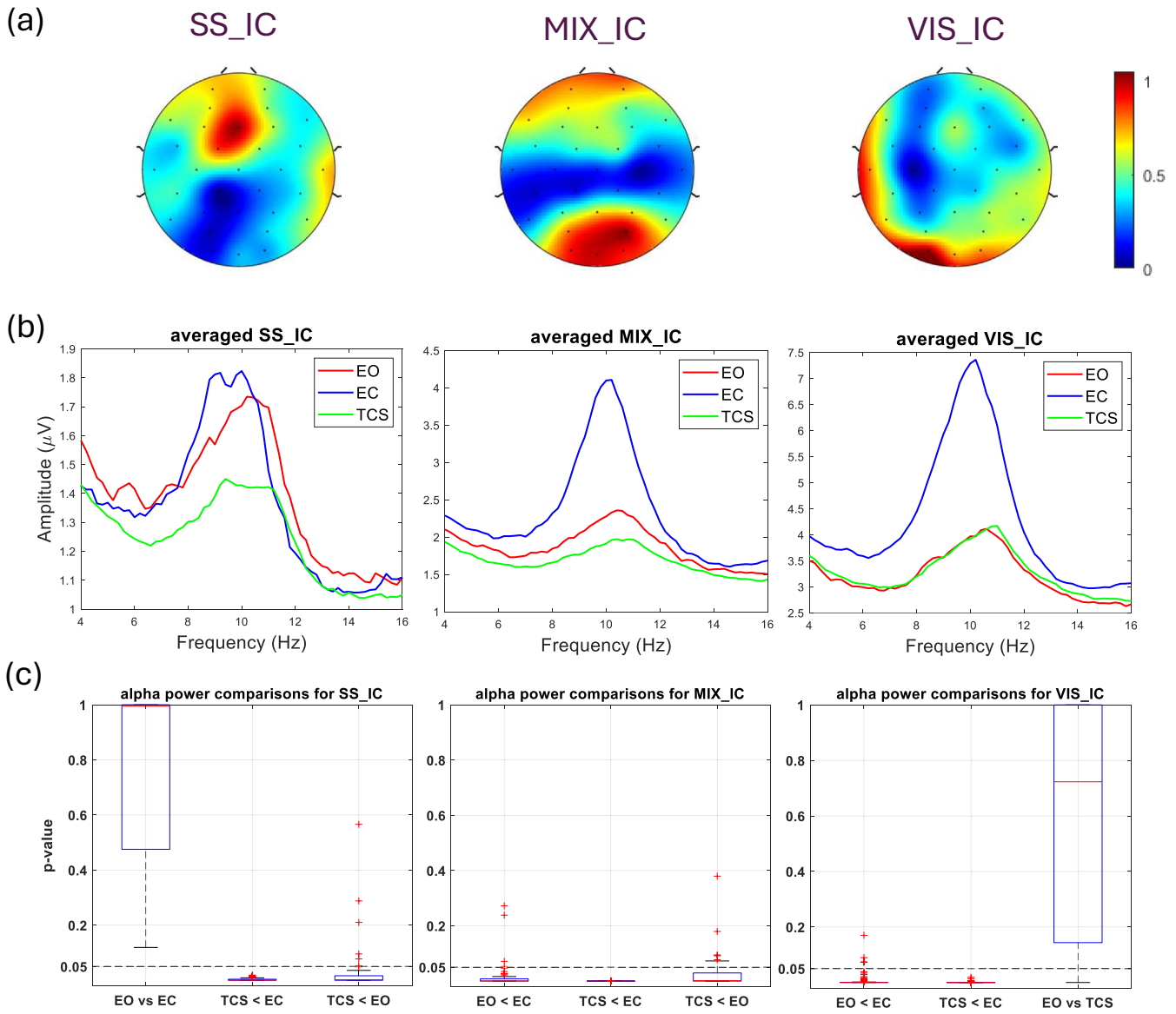

FIGURE 8 | Quantification analyses for identified components based on the presented algorithm. (a) Spatial weight topography of the selected IAF ICs, showing the contribution of each channel to the components mixing matrix derived from ICA. (b) Averaged spectral pattern of identified components for different conditions. (c) Distribution of *p* values resulted from alpha power comparison across different conditions. EC, eyes closed; EO, eyes open; TCS, thermal cutaneous stimulation.

frequency during the experiment (close to the overall mean IAF of 10.02 Hz and SS-IAF mean of 9.99 Hz). Figure 8 shows quantification analyses for identified components. Figure 8a shows how different channels contributed to extract SS-IC, MIX-IC and VIS-IC. Averages of the spectral patterns for the identified components under different conditions are illustrated in Figure 8b. We performed pairwise *t*-tests (Bonferroni corrected for multiple comparisons) to compare the alpha power of these identified components across different conditions. Figure 8c shows the distribution of *p* values for each comparison.

In Figure 9, the average alpha spectral pattern across participants is illustrated, revealing greater fluctuations postsham compared to presham than the fluctuations observed postactive compared to preactive. Specifically, during SS-IAF tACS, the IAF remained more stable, showing minimal deviation from its prestimulation frequency. In contrast, during sham, the IAF shifted towards lower frequencies in the same participants. The distribution of the selected IAF across participants is presented in Figure 10. Comparing overall selected IAF at the C3/C4 location across conditions and time using LMM showed no significant changes across conditions or time points. When considering only SS-tACS-IAF, a marginal time effect ($F = 3.9$, $p = 0.05$) and a trend towards an interaction for the postactive condition ($F = 3.2$, $p = 0.07$) were observed.

Figure 11 provides a detailed view of how tACS at SS-IAF affects HPT. Correlation analyses reveal that a significant correlation exists between SS-IAF variations and HPT for the sham condition ($R = 0.44$, $p = 0.03$), indicating that a decrease in IAF is associated with a decrease in HPT. However, no such correlation is observed for the tACS condition.

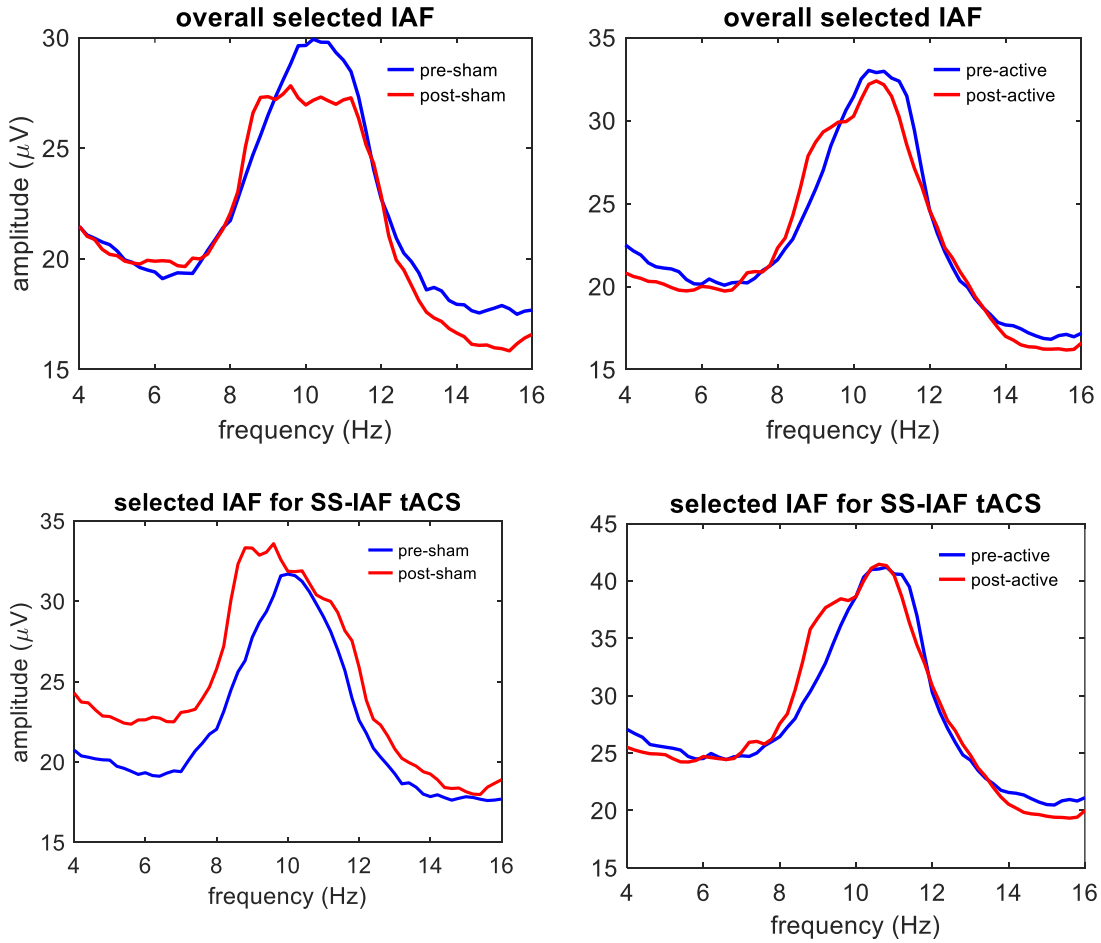

FIGURE 9 | Alpha spectral pattern averaged across all participants for each condition. A clear shift can be seen for postsham SS-IAF compared to presham SS-IAF.

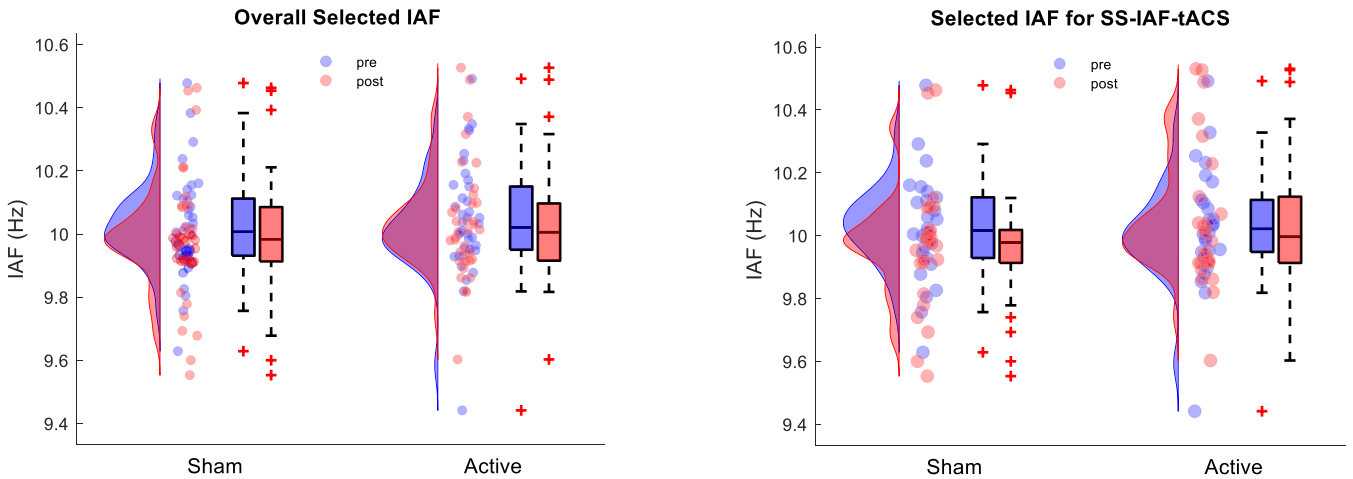

FIGURE 10 | Selected IAF at the C3/C4 location across experimental conditions and time points. LMM analysis revealed no significant differences between conditions ($p = 0.38$), time points ($p = 0.14$) or their interaction ($p = 0.51$) for the overall selected IAF across all participants ($n = 38$). However, for those who received tACS at SS-IAF ($n = 26$), a marginal time effect ($F = 3.9$, $p = 0.05$) and a trend toward an interaction for the postactive condition ($F = 3.2$, $p = 0.07$) were observed.

3.5 | Exploring the Effects of SS-IAF and Sex on Behavioural Response to the tACS

We performed exploratory analyses to investigate how sex may influence the behavioural response to tACS. While the sample size for each subgroup (female/male/SS-IAF) is not sufficient to draw definitive conclusions, these analyses were intended to identify potential trends and define directions for future research. The results in Figure 12 (with statistical tests results in Tables S1 and S2) indicate that, in general, the time effect on

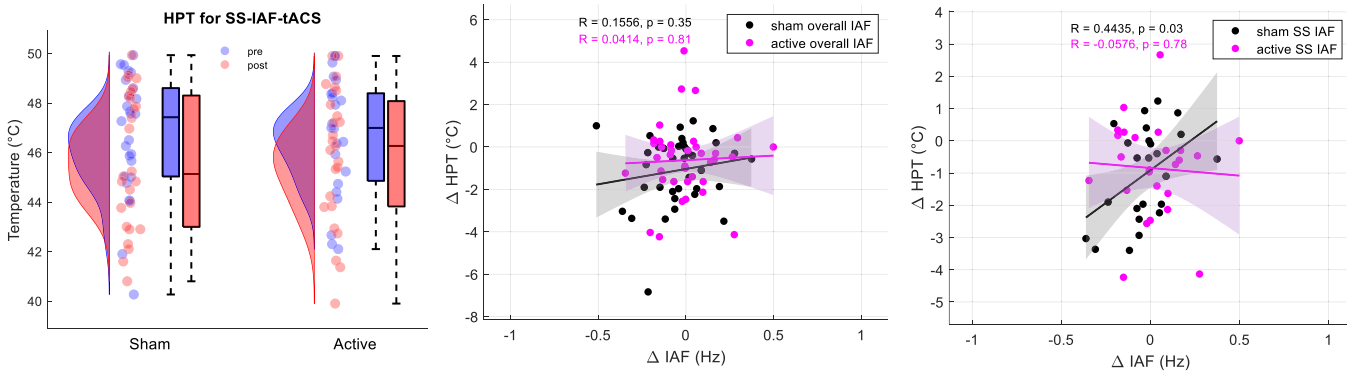

FIGURE 11 | HPT relationship with IAF. Left: Distribution of HPT (°C) pre- and poststimulation across all conditions for participants who received SS-IAF tACS. A significant time effect was observed ($F = 9.3$, $p = 0.003$), but no interaction ($p = 0.47$) or condition effect ($p = 0.71$). Middle and right: Correlation analyses between changes in IAF (Δ IAF) and changes in HPT (Δ HPT) for overall IAF (middle) and SS-IAF (right). A significant correlation between Δ SS-IAF and Δ HPT was found for the sham condition ($R = 0.44$, $p = 0.03$), indicating that a decrease in IAF is associated with a decrease in HPT, whereas no such correlation was observed for the tACS condition.

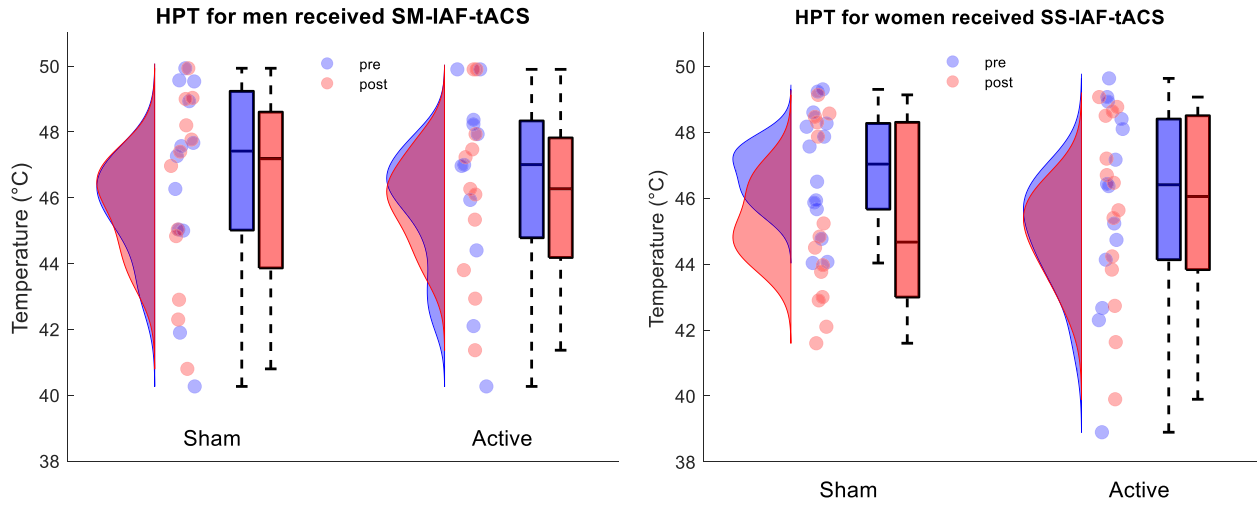

FIGURE 12 | HPT distribution for men (left) and women (right) who received tACS at SS-IAF ($n = 12$ for men, $n = 14$ for women).

behavioural measures was stronger in females than in males. Specifically, no significant time effect was observed for HPT in males, whereas a significant time effect was found for HPT in females. Additionally, a trend was observed in females, suggesting greater postactive tACS effects compared to postsham conditions.

4 | Discussion

In this study, we examined how individualised alpha-tACS applied to M1 affects neural oscillations and behavioural responses to sustained thermonociceptive stimuli in healthy participants. In this section, we discuss each of our hypotheses based on the observed results of the previous section.

4.1 | Sensory Sensations Associated With tACS and Sham

Although both the experimenter and participants were blinded to the protocol (sham or active) and experimental parameters, participants reported different sensory perceptions between the two conditions. It is important to underline that although participants perceived sham and tACS conditions differently, they remained unaware of the study's true objectives. Crucially, the use of HPT and WDT measurements in this study helped mitigate the bias, as participants were unaware of the exact temperature of the stimulation they received. Instead, they responded purely based on their perceived pain or warmth sensation without explicit knowledge of the stimulation intensity. Additionally, the marginal differences observed in this study were specific to certain subgroups, such as male versus female participants or those receiving tACS at SS-IAF. If bias had influenced responses, participants would have likely reported a direct pain reduction after tACS rather than a moderated increase for both tACS and sham.

4.2 | Individualised tACS and Pain Perception

The decreased WDT and HPT values in the post-tACS phase suggest mild sensitisation of the forearm, which could also account for the increased ratings of sustained thermonociceptive stimuli.

While the average values showed that tACS resulted in a less pronounced decrease in WDT and HPT, as well as a smaller

increase in intensity and painfulness ratings compared to sham, these differences were not statistically significant. Nevertheless, the consistency of these trends across the different behavioural measures suggests a potential modulatory effect of tACS on nociceptive processing and pain perception.

As a potential source of variability in pain perception, we conducted an exploratory analysis to examine the influence of sex on tACS modulation of behavioural responses. Overall, the comparison of postphase to prephase revealed a more pronounced effect in women than in men, with HPT showing the most significant decrease over time in women and no significant change in men. Additionally, there was a trend for an interaction effect, indicating that females responded better to tACS at SS-IAF. Sex and gender differences in pain perception and sensitivity have been widely documented, with females generally showing higher pain sensitivity compared to males (Osborne and Davis 2022; Stratton et al. 2024). These differences may stem from hormonal, immune and structural variations in nociceptive pathways. Regarding tACS or transcranial electrical stimulation (tES) in general, while research on sex differences is limited, anatomical differences, such as skull thickness and brain morphology, along with physiological factors like hormonal fluctuations, can influence the distribution and efficacy of electrical current during stimulation (Bhattacharjee et al. 2022; Krause and Kadosh 2014; Weller et al. 2023; Zanto et al. 2021). Adapting tES protocols to account for these factors could enhance the effectiveness of neuromodulation across diverse populations. These factors are also likely contributors to individual variability in IAF (Bazanova et al. 2014), further emphasising the need for personalised approaches.

4.3 | Neural Phase-Locked and Ongoing Oscillations Responses During Sustained Periodic Thermonociceptive Stimuli to tACS

Frequency-tagging analysis revealed significant phase-locked modulations in frontal-central electrodes in response to periodic thermonociceptive stimuli, as well as in central and posterior-central areas for theta, and in central and parietal regions contralateral to the dominant arm for alpha and beta, consistent with previous findings in the literature (Colon et al. 2017; Leu et al. 2023). Statistical tests on amplitude variations at the frequency of interest (0.2 Hz) and its harmonics showed no significant effects of time or condition on ongoing neural oscillations during sustained thermonociceptive stimulation. However, phase-locked responses significantly decreased in the poststimulation phase compared to the prestimulation phase, regardless of condition. While no tACS effect was found on PL amplitude, the reduction in the 'post' phase may be linked to habituation to the periodic aspect of the stimuli (Liberati, Algoet, Klöcker, et al. 2018; Mulders et al. 2020). Moreover, exploratory analyses (see Table S2) showed marginal tACS effects when using SS-IAF. This highlights the need for more personalised and optimised stimulation protocols.

4.4 | tACS Effects on IAF and the Relationship Between IAF and Pain Perception

A key methodological distinction of the current study is using a component-based task-induced approach to detect SS-IAF. This method prioritised functional reactivity to thermal stimulation over anatomical localisation to ensure relevance to the pain-processing context. Stringent criteria limited the number of identifiable SS-IC. Future studies could adopt a more flexible approach by tailoring CI to different selection criteria.

Comparing overall selected IAF values revealed no significant change in overall selected IAF; however, SS-IAF significantly decreased in the post phase compared to the pre phase regardless of condition. The correlation analysis showed a positive relationship between ΔHPT and ΔSS-IAF, indicating that higher sensitivity is associated with slower alpha frequencies. When analysing the correlation between ΔSS-IAF and ΔHPT separately for the active and sham conditions, a significant correlation was observed only in the sham condition, with no correlation in the active condition.

The observed positive correlation between ΔHPT and ΔSS-IAF is consistent with the relationship between IAF and pain perception observed in chronic pain patients (Furman et al. 2019; Sarnthein et al. 2006; de Vries et al. 2013; Walton et al. 2010) and some experimental pain studies (Furman et al. 2018, 2020, 2024; Chowdhury et al. 2025). On the other hand, May et al. assessed the predictive value of IAF for sensitivity to brief experimental pain, finding that variations in pain perception were not consistently predicted by IAF, indicating that the relationship between IAF and pain may not generalise to all types of pain (May et al. 2025). While IAF holds promise as a biomarker for pain sensitivity, these mixed findings could also stem from several factors such as methodological variations in IAF estimation and differences between sensor-based and component space-based methods. As has been shown previously, central and sensorimotor component (Furman et al. 2018; Chowdhury et al. 2025) might better index pain sensitivity than sensor-based methods (May et al. 2025).

4.5 | Concluding Remarks and Future Directions

Although the effect of individualised tACS on pain perception did not reach statistical significance, the consistent trends observed indicate a potential modulatory role that calls for further exploration. Future studies should enhance the personalisation of tACS by considering individual variability and condition- or state-dependent factors. Multiple potential biomarkers of pain sensitivity, such as hormonal or structural factors, should be taken into account. Finally, future research should investigate the effects of individualised tACS in clinical populations to evaluate its therapeutic potential while also assessing its long-term effects.

Author Contributions

Conceptualisation, methodology, writing – original draft: Y.F. and G.L. Data collection: Y.F. and F.D. Data analyses: Y.F. and G.R. Writing – review and editing: Y.F., F.D., G.R. and G.L. Supervision, project administration, funding acquisition: G.L. All authors discussed the results and commented on the manuscript.

Acknowledgements

Y.F. is supported by a MIS grant from the FNRS, and G.L. is supported by FNRS and Fondation Médicale Reine Elisabeth (FMRE) grants. We wish to thank all the members of the Nocions Lab (http://nocions.org) for the useful discussions and the CATL team of our department for

technical assistance. In particular, we would like to express our gratitude to André Mouraux and Louisien Lebrun for sharing their valuable opinions on the methodology. No generative AI or AI-assisted technologies were used in the preparation of this manuscript.

Conflicts of Interest

The authors declare no conflicts of interest.

Data Availability Statement

The data and code are available via reasonable requests to the corresponding author.

References

Ali, M. M., K. K. Sellers, and F. Fröhlich. 2013. "Transcranial Alternating Current Stimulation Modulates Large-Scale Cortical Network Activity by Network Resonance." *Journal of Neuroscience* 33: 11262–11275.

Arendsen, L. J., S. Hugh-Jones, and D. M. Lloyd. 2018. "Transcranial Alternating Current Stimulation at Alpha Frequency Reduces Pain When the Intensity of Pain Is Uncertain." *Journal of Pain* 19: 807–818.

Bazanova, O. M., A. V. Kondratenko, O. I. Kuzminova, K. B. Muravlyova, and S. E. Petrova. 2014. "EEG Alpha Indices Depending on the Menstrual Cycle Phase and Salivary Progesterone Level." *Human Physiology* 40: 140–148.

Bhattacharjee, S., R. Kashyap, A. M. Goodwill, et al. 2022. "Sex Difference in tDCS Current Mediated by Changes in Cortical Anatomy: A Study Across Young, Middle and Older Adults." *Brain Stimulation* 15: 125–140.

Castellanos, N. P., and V. A. Makarov. 2006. "Recovering EEG Brain Signals: Artifact Suppression With Wavelet Enhanced Independent Component Analysis." *Journal of Neuroscience Methods* 158: 300–312.

Chowdhury, N. S., C. Bi, A. J. Furman, et al. 2025. "Predicting Individual Pain Sensitivity Using a Novel Cortical Biomarker Signature." *JAMA Neurology* 82: 237–246.

Colon, E., G. Liberati, and A. Mouraux. 2017. "EEG Frequency Tagging Using Ultra-Slow Periodic Heat Stimulation of the Skin Reveals Cortical Activity Specifically Related to C Fiber Thermonociceptors." *NeuroImage* 146: 266–274.

de Vries, M., O. H. G. Wilder-Smith, M. L. A. Jongsma, et al. 2013. "Altered Resting State EEG in Chronic Pancreatitis Patients: Toward a Marker for Chronic Pain." *Journal of Pain Research* 6: 815–824.

Furman, A. J., T. J. Meeker, J. C. Rietschel, et al. 2018. "Cerebral Peak Alpha Frequency Predicts Individual Differences in Pain Sensitivity." *NeuroImage* 167: 203–210.

Furman, A. J., M. Prokhorenko, M. L. Keaser, et al. 2020. "Sensorimotor Peak Alpha Frequency Is a Reliable Biomarker of Pain Sensitivity." *BioRxiv* 613299: 6069–6082.

Furman, A. J., M. Prokhorenko, M. L. Keaser, et al. 2024. "Prolonged Pain Reliably Slows Peak Alpha Frequency by Reducing Fast Alpha Power." *eLife* 13: RP102096.

Furman, A. J., T. Thapa, S. J. Summers, et al. 2019. "Cerebral Peak Alpha Frequency Reflects Average Pain Severity in a Human Model of Sustained, Musculoskeletal Pain." *Journal of Neurophysiology* 122: 1784–1793.

Garakh, Z., V. Novototsky-Vlasov, E. Larionova, and Y. Zaytseva. 2020. "Mu Rhythm Separation From the Mix With Alpha Rhythm: Principal Component Analyses and Factor Topography." *Journal of Neuroscience Methods* 346: 108892.

Gundlach, C., M. M. Müller, T. Nierhaus, A. Villringer, and B. Sehm. 2017. "Modulation of Somatosensory Alpha Rhythm by Transcranial Alternating Current Stimulation at Mu-Frequency." *Frontiers in Human Neuroscience* 11: 432.

Hohn, V. D., L. Tiemann, F. S. Bott, et al. 2025. "Neurofeedback and Attention Modulate Somatosensory Alpha Oscillations but Not Pain Perception." *PLoS Biology* 23: e3002972.

Huang, W. A., I. M. Stitt, E. Negahbani, et al. 2021. "Transcranial Alternating Current Stimulation Entrains Alpha Oscillations by Preferential Phase Synchronization of Fast-Spiking Cortical Neurons to Stimulation Waveform." *Nature Communications* 12: 3151.

Huber, F. A., P. A. Kell, J. O. Shadlow, and J. L. Rhudy. 2025. "Cerebral Peak Alpha Frequency: Associations With Chronic Pain Onset and Pain Modulation." *Neurobiology of Pain* 18: 100180.

Huneke, N. T. M., C. A. Brown, E. Burford, et al. 2013. "Experimental Placebo Analgesia Changes Resting-State Alpha Oscillations." *PLoS One* 8: e78278.

Krause, B., and R. C. Kadosh. 2014. "Not All Brains Are Created Equal: The Relevance of Individual Differences in Responsiveness to Transcranial Electrical Stimulation." *Frontiers in Systems Neuroscience* 8: 76558.

Lebrun, L., G. Ricci, A. Courtin, E. N. van den Broeke, C. Lenoir, and A. Mouraux. 2025. "Interindividual Variations in Peak Alpha Frequency Do Not Predict the Magnitude or Extent of Secondary Hyperalgesia Induced by High-Frequency Stimulation." *bioRxiv*, 2025.06.02.657417.

Leu, C., A. Courtin, C. Cussac, and G. Liberati. 2023. "The Role of Ongoing Oscillation in Pain Perception: Absence of Modulation by a Concomitant Arithmetic Task." *Cortex* 168: 114–129.

Leu, C., E. Glineur, and G. Liberati. 2024. "Cue-Based Modulation of Pain Stimulus Expectation: Do Ongoing Oscillations Reflect Changes in Pain Perception? A Registered Report." *Royal Society Open Science* 11: 240626.

Liberati, G., M. Algoet, S. Ferrao Santos, J. G. Ribeiro-Vaz, C. Raftopoulos, and A. Mouraux. 2018. "Thermonociceptive Stimuli Preferentially Modulate Theta and Alpha Oscillations in the Human Posterior Insula: Evidence From Intracerebral Recordings." *Frontiers in Neuroscience* 12.

Liberati, G., M. Algoet, A. Klöcker, et al. 2018. "Habituation of Phase-Locked Local Field Potentials and Gamma-Band Oscillations Recorded From the Human Insula." *Scientific Reports* 8: 1–13.

Liberati, G., M. Algoet, S. F. Santos, J. G. Ribeiro-Vaz, C. Raftopoulos, and A. Mouraux. 2019. "Tonic Thermonociceptive Stimulation Selectively Modulates Ongoing Neural Oscillations in the Human Posterior Insula: Evidence From Intracerebral EEG." *NeuroImage* 188: 70–83.

Liberati, G., A. Klöcker, M. Algoet, et al. 2018. "Gamma-Band Oscillations Preferential for Nociception Can Be Recorded in the Human Insula." *Cerebral Cortex* 28: 3650–3664.

May, E. S., M. Butz, N. Kahlbrock, N. Hoogenboom, M. Brenner, and A. Schnitzler. 2012. "Pre- and Post-Stimulus Alpha Activity Shows Differential Modulation With Spatial Attention During the Processing of Pain." *NeuroImage* 62: 1965–1974.

May, E. S., L. Tiemann, C. Gil Ávila, et al. 2025. "Assessing the Predictive Value of Peak Alpha Frequency for the Sensitivity to Pain." *Pain*, Ahead of Print.

Mazaheri, A., D. A. Seminowicz, and A. J. Furman. 2022. "Peak Alpha Frequency as a Candidate Biomarker of Pain Sensitivity: The Importance of Distinguishing Slow From Slowing." *NeuroImage* 262: 119560.

McLain, N. J., M. S. Yani, and J. J. Kutch. 2022. "Analytic Consistency and Neural Correlates of Peak Alpha Frequency in the Study of Pain." *Journal of Neuroscience Methods* 368: 109460.

Mulders, D., C. de Bodt, N. Lejeune, et al. 2020. "Dynamics of the Perception and EEG Signals Triggered by Tonic Warm and Cool Stimulation." *PLoS One* 15: 1–25.

Murray, G. M., and B. J. Sessle. 2024. "Pain-Sensorimotor Interactions: New Perspectives and a New Model." *Neurobiology of Pain* 15: 100150.

Nir, R. R., A. Sinai, R. Moont, E. Harari, and D. Yarnitsky. 2012. "Tonic Pain and Continuous EEG: Prediction of Subjective Pain Perception by Alpha-1 Power During Stimulation and at Rest." *Clinical Neurophysiology* 123: 605–612.

Osborne, N. R., and K. D. Davis. 2022. "Sex and Gender Differences in Pain." *International Review of Neurobiology* 164: 277–307.

Pernet, C., M. I. Garrido, A. Gramfort, et al. 2020. "Issues and Recommendations From the OHBM COBIDAS MEEG Committee for Reproducible EEG and MEG Research." *Nature Neuroscience* 23: 1473–1483.

Ploner, M., C. Sorg, and J. Gross. 2017. "Brain Rhythms of Pain." *Trends in Cognitive Sciences* 21: 100–110.

Riddle, J., and F. Frohlich. 2021. "Targeting Neural Oscillations With Transcranial Alternating Current Stimulation." *Brain Research* 1765: 147491.

Sarnthein, J., J. Stern, C. Aufenberg, V. Rousson, and D. Jeanmonod. 2006. "Increased EEG Power and Slowed Dominant Frequency in Patients With Neurogenic Pain." *Brain* 129: 55–64.

Sorokin, J. 2025. "wICA(Data, Varargin)."

Stratton, H., G. Lee, M. Dolatyari, et al. 2024. "Nociceptors Are Functionally Male or Female: From Mouse to Monkey to Man." *Brain* 147: 4280–4291.

Vossen, A., J. Gross, and G. Thut. 2015. "Alpha Power Increase After Transcranial Alternating Current Stimulation at Alpha Frequency (a-tACS) Reflects Plastic Changes Rather Than Entrainment." *Brain Stimulation* 8: 499–508.

Walton, K. D., M. Dubois, and R. R. Llinás. 2010. "Abnormal Thalamocortical Activity in Patients With Complex Regional Pain Syndrome (CRPS) Type I." *Pain* 150: 41–51.

Weller, S., B. Derntl, and C. Plewnia. 2023. "Sex Matters for the Enhancement of Cognitive Training With Transcranial Direct Current Stimulation (tDCS)." *Biology of Sex Differences* 14: 78.

Zanto, T. P., K. T. Jones, A. E. Ostrand, W.-Y. Hsu, R. Campusano, and A. Gazzaley. 2021. "Individual Differences in Neuroanatomy and Neurophysiology Predict Effects of Transcranial Alternating Current Stimulation." *Brain Stimulation* 14: 1317–1329.

Supporting Information

Additional supporting information can be found online in the Supporting Information section.